

SOLIDS AND LIQUIDS

Features and Mechanisms of the Generation of Neutrons and Other Particles in First Laser Fusion Experiments

V. I. Vysotskii^{a,*}, A. A. Kornilova^b, and M. V. Vysotskiy^a

^a Taras Shevchenko National University of Kyiv, Kyiv, 01033 Ukraine

^b Moscow State University, Moscow, 119991 Russia

* e-mail: vivysotskii@gmail.com

Received March 24, 2020; revised April 23, 2020; accepted May 11, 2020

Abstract—The quantitative characteristics of the first successful experiments on the formation of a fusion plasma have been discussed. It has been shown that the generation of neutrons detected in these experiments is not directly due to fusion processes in a laser plasma with a comparatively low temperature. Alternative mechanisms of stimulation of a fusion reaction have been considered. It has been shown that the most probable mechanism of neutron generation is attributed to the processes of formation of correlated coherent states, which are generated by a shock wave in the undestroyed part of the target lattice or at the motion of slow ions emitted from the laser plasma in the target. It is reasonable to repeat these experiments, where the effective generation of not only neutrons but also other products of nuclear fusion should be expected.

DOI: 10.1134/S1063776120090101

1. INTRODUCTION

The first successful experiments on nuclear fusion stimulated by the laser action on a target were performed in the late 1960s [1–3]. For those experiments, single short (durations of about 10^{-11} s) optical pulses were generated by a high-power neodymium laser with a wavelength of $1.06 \mu\text{m}$. The energy of each pulse reached 10 J and ensured a radiation intensity of $J \approx 10^{16} \text{ W/cm}^2$. At that time, these parameters were among the worldwide-best parameters.

Such laser pulses were focused in vacuum by a long-focus lens on the surface of a LiD target; as a result, an unsteady plasma was formed. The aim of those experiments was to detect fusion neutrons generated in the bulk of this plasma synchronously with the pulse. Fast neutrons were detected by a scintillation counter based on a unique $(\text{CH}_2)_n$ polystyrene crystal with the diameter $D = 30 \text{ cm}$ and the length $L = 20 \text{ cm}$ placed at the distance $R = 10 \text{ cm}$ from the region of action of the laser pulse. For these parameters, the solid angle of neutron detection was

$$\Delta\Omega = 2\pi \sqrt{1 - \frac{R^2}{R^2 + (D/2)^2}} \approx 1.3\pi.$$

Taking into account the geometry of location of the detector and a number of other parameters, the authors estimated the total efficiency of neutron detection as $\eta \approx 10\%$.

According to the data obtained in [1, 2], one neutron per laser pulse was detected on average under this

action. These data were interpreted as confirmation of nuclear fusion (in fact, as the first demonstration of laser inertial confinement fusion) through the following one of the three channels of the dd reaction:

$$d + d = \text{He}^3 + n + 3.27 \text{ MeV}, \quad (1)$$

which occurs at collisions of deuterons in the heated plasma formed in the region of the laser focus on the target surface.

The analysis performed in [1–3] was based on the following characteristics of the formed plasma: the deuterium ion density $n_d \approx 10^{21} \text{ cm}^{-3}$, the thickness of the plasma region near the laser focus $x_0 \approx 10^{-2} \text{ cm}$, the maximum ion temperature of the plasma $kT \approx 120 \text{ eV}$ and $kT = 210 \text{ eV}$ for the spherical and planar geometries of its expansion, respectively (see [3], Fig. 10), and the time of plasma existence with this temperature $\tau \approx 5 \times 10^{-10} \text{ s}$. The rms velocity of deuterium ions in the plasma at the maximum temperature was $\langle v \rangle \approx \sqrt{3kT/M} \approx 10^7 \text{ cm/s}$.

The area of the transverse expansion of the plasma in this time (taking into account the initial cross section of the focused laser pulse $S_0 = \pi R_0^2 \approx 3 \times 10^{-4} \text{ cm}^2$) was

$$S_\tau \approx \pi(\langle v \rangle \tau + R_0)^2 \approx 6 \times 10^{-4} \text{ cm}^2.$$

According to these parameters, the number of deuterons in the bulk of the plasma was $N_d = n_0 S_\tau x_0 \approx 6 \times 10^{15}$.

After the description of the plasma and its analysis, the authors of [1–3] stated that the results of the experiments are in agreement with calculations and confirm the expected detection of neutrons from laser-induced nuclear fusion. It is noteworthy that the authors of [1–3] performed the appropriate detailed study of the characteristics of laser pulses and the process of formation of the plasma, but they almost did not consider features of nuclear fusion. We perform this analysis in this work.

2. ESTIMATES OF THE EFFICIENCY OF FUSION UNDER THE ACTION OF A SINGLE LASER PULSE

The total number of the dd reaction events involving all deuterons in the laser plasma volume in the time of its existence (and, thereby, the total number of neutrons generated in nuclear fusion in the region of action of the laser pulse) can be calculated by the standard formula

$$N_{\text{neutron}}^0 \approx N_0^2 \langle \sigma(v)v \rangle \tau / 2, \quad (2)$$

which includes the product of the reaction cross section $\sigma(v)$ and the velocity of involved particles averaged over the Maxwellian distribution. This product for the case of the dd reaction given by Eq. (1) with the yield of neutrons is given by the well-known expression ([4, Chapter 2])

$$\langle \sigma(v)v \rangle_{dd} \approx 1.3 \times 10^{-14} \frac{1}{(kT)^{2/3}} \exp\left(-\frac{18.8}{(kT)^{1/3}}\right) \left[\frac{\text{cm}^3}{\text{s}}\right], \quad (3)$$

where kT is the plasma temperature in keV.

Taking into account that the spatial shape of plasma expansion was close to spherical ([3, Fig. 2]) and setting its ion temperature to the maximum value $kT \approx 130$ eV, we find from Eq. (3) that $\langle \sigma(v)v \rangle \approx 5 \times 10^{-30} \text{ cm}^3/\text{s}$ for this configuration [3]. With this value, the average number of neutrons generated in the LiD target irradiated by a single laser pulse in the experiments reported in [1, 2] can be determined from Eq. (2) as

$$N_{\text{neutron}}^0 \approx 0.007 \text{ neutron/pulse}. \quad (4)$$

According to this estimate, the generation (not detection!) of at least one neutron in the nuclear fusion reaction (1) in the discussed experiment requires the successive action of about 150 laser pulses. This is inconsistent with the results of the experiments reported in [1, 2], where for the experimental efficiency of detection $N_{\text{neutron}} \approx 1$ neutron/pulse, the efficiency of their generation in reaction (1) should be

$$N_{\text{neutron}}^0 \approx N_{\text{neutron}} / \eta \approx 10 \text{ neutron/pulse}, \quad (5)$$

which is a factor of 1500 higher than the efficiency that can be ensured by nuclear fusion in the experiments reported in [1, 2].

From the above estimates, it is obvious that neutrons detected in those experiments could not be produced only from nuclear fusion in the volume of the plasma formed under the action of the laser pulse on the surface of the LiD target. We have no doubt in high qualification of the authors of [1–3] and in the correctness of their measurements, but a question arises: What is the origin of neutrons detected in those experiments?

3. POSSIBLE MECHANISM OF NEUTRON GENERATION AND CONDITIONS FOR THE GENERATION OF OTHER PARTICLES IN THE LiD TARGET IRRADIATED BY A LASER PULSE

We believe that neutrons detected in the experiments were generated in low-energy nuclear reactions, which were stimulated by side effects, which are not directly related to an increase in the temperature and accompany the action of laser pulses on the surface of targets.

We emphasize two main mechanisms that are based on the same physical process and result in effective nuclear fusion.

The first mechanism is due to a shock wave appearing under the action of the laser pulse on a target. It is well known that this action always leads to the ablation caused by the intense pulsed evaporation of fast ions from the part of the target surface subjected to the laser pulse. This evaporation is accompanied by the momentum transfer to the target, which results in the formation of an intense shock wave moving into the target normally to its surface.

This process actually corresponds to the principle of operation of any jet engine accelerated by means of the ejection of mass in the opposite direction. This mechanism of generation of shock waves is well known [5–9].

The characteristic shock pressure under such ablation on the remaining (unevaporated) part of the target is $P \approx 4 \times 10^6$ atm at the intensity of the laser pulse $J = 10^{13} \text{ W/cm}^2$ [5], which is equivalent to, e.g., the collision of a micrometeorite with a size of several micron moving at a velocity of 13 km/s with the target. As the intensity of the laser pulse increases, the pressure increases sharply as $P \propto J^{7/9}$ [8, 9], reaching giant values $P \approx 10^8$ – 10^9 atm at the intensity $J \approx 10^{16} \text{ W/cm}^2$ corresponding to this experiment.

The velocity of the shock front generated at the ablation with the above parameters of the laser pulse can reach or exceed 4–8 km/s. The motion of the shock wave inside any material bodies is accompanied by a very sharp narrowing of its leading front to a size whose minimum value is several nanometers. Such a

steepening of the shock front occurs because the more intense (main) part of the shock front moves faster than the less intense leading part of the front and “overtakes” it owing to the nonlinearity of the interaction.

The passage of this shock wave through the target containing deuterium and lithium results in a very fast (duration of 10^{-13} – 10^{-11} s) shock compression and, then, to fast expansion and subsequent slower relaxation of the local environment of each of the deuterium and lithium atoms in the target. In terms of the dynamics of ions of the crystal lattice, this corresponds to a very rapid pulsed reversible modulation of the parameters (in particular, the frequency of oscillations) of a time-dependent harmonic oscillator characterizing a vibrational state (including optical phonon modes at frequencies of 10–15 THz) of each of the deuteron in the lattice. This very fast process of nonstationary modulation leads to the phase matching of optical phonon modes and to the formation of the correlated coherent state of these nuclei. As a result, giant fluctuations of the momentum and energy of these nuclei corresponding to these states are generated [10–17].

Such a mechanism of pulsed modulation of the parameters of the local oscillator will be particularly efficient in the region adjacent to the region of formation of the laser plasma. Numerous nanocracks appear in this region already before the arrival of the shock wave; these nanocracks are formed owing to the fast ions entering this region from the volume of the formed surface plasma. This process is similar to the cracking of metallic hydrides such as TiD or TiH at their saturation with hydrogen isotopes. A comparatively large width of these nanocracks filled with deuterium very strongly (by several times) increases the amplitude of the possible modulation of the frequency of deuteron oscillations at the subsequent action of the shock wave on these nanocracks. An additional consequence of the action of the shock wave is the rapid “opening” of nanocracks that have not yet been formed but were in a very stressed state because of the internal pressure of deuterons entering an interstice of the lattice of the target.

Just such conditions of the fast modulation of the equivalent oscillator are required to efficiently form the correlated coherent state of these deuterons.

It was shown in [10–17] that the amplitude of fluctuations of the kinetic energy of the particle (e.g., proton) under such pulsed modulation of the parameters of the nonstationary oscillator can reach δE_{corr} in the range of 10–30 keV even in the case of the crystal lattice at room temperature. It is very interesting that the average kinetic energy of these nuclei can remain constantly small and differ slightly from the thermal energy of the condensed target!

It is important that giant energy fluctuations in such correlated coherent states will always exist for an

anomalously large time δt_{corr} , which is many orders of magnitude larger than the duration of uncorrelated fluctuations δt_{uncorr} , if it is estimated from the “ordinary” Heisenberg uncertainty relation $\delta t_{\text{uncorr}} \approx \hbar/2\delta E$.

The possibility of the existence of such correlated coherent states was justified in the general form (for various pairs of arbitrary dynamic variables A and B) in 1930 independently by Schrödinger and Robertson [18, 19] on the basis of the general rules of quantum mechanics. In the general case, these relations are characterized by the generalized uncertainty relations for the variance of these variables with the explicit form of their operators \hat{A} , \hat{B} , and \hat{C} :

$$\begin{aligned}\sigma_A \sigma_B &\equiv (\delta A)^2 (\delta B)^2 \geq \frac{|\langle [\hat{A}, \hat{B}] \rangle|^2}{4(1 - r_{AB}^2)}, \\ \sigma_C &= \langle (\hat{C} - \langle C \rangle)^2 \rangle, \quad r_{AB} = \frac{\sigma_{AB}}{\sqrt{\sigma_A \sigma_B}}, \\ \sigma_{AB} &= \frac{\langle \hat{A} \hat{B} + \hat{B} \hat{A} \rangle}{2} - \langle A \rangle \langle B \rangle, \quad |r_{AB}| \leq 1.\end{aligned}\quad (6)$$

In particular, this state for the coordinate–momentum variable pair is characterized by the Schrödinger–Robertson uncertainty relation different from the Heisenberg uncertainty relation:

$$\delta p \delta x \geq \hbar/2\sqrt{1 - r^2} \equiv \hbar G/2, \quad (7)$$

where $0 \leq |r| < 1$ and $1 \leq G < \infty$ are the correlation coefficient and the coefficient of correlation efficiency, respectively. These coefficients characterize the phase-matching degree and mutual correlation of different eigenstates of a particle in a superpose quantum state (in particular, phase matching of vibrational modes of the deuteron in the space between neighboring lithium atoms in the lattice).

For uncorrelated states, $r = 0$ and $G = 1$, whereas for correlated states, $|r| \rightarrow 1$ and $G \gg 1$. The characteristics of these states and the possibility of their application were studied in many works (in particular, see reviews [20, 21]).

A fundamental difference of the interaction of particles with very large fluctuations of the momentum (and, thereby, fluctuations of the kinetic energy) from the interaction of particles with the real (not virtual) kinetic energy similar in magnitude is that particles with the virtual energy cannot, e.g., ensure endoenergetic reactions, excite (ionize) other atoms or generate bremsstrahlung because such processes are accompanied by the irreversible energy loss, which is fundamentally forbidden for virtual fluctuations of the energy associated with its uncertainty and the general energy conservation law, which will be satisfied after the vanishing of fluctuations.

At the same time, such particles can “involve” a large momentum fluctuation δp and, correspondingly, fluctuation of the virtual kinetic energy $\delta E = (\delta p)^2/2M$ at correlated coherent states for, e.g., the passage

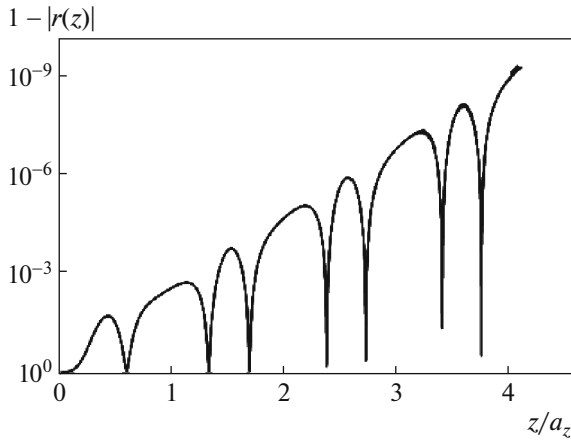


Fig. 1. Formation of a correlated coherent state at the motion of protons with an optimal energy of 450–500 eV in a lithium crystal in the planar channeling regime in the z direction (a_z is the longitudinal period of the lithium lattice).

through the potential barrier and the subsequent stimulation of nuclear or chemical reactions if they are exoenergetic.

This mechanism based on the pulsed modulation of the parameters of local harmonic oscillators under the action of the shock wave successfully explains the results of experiments on the generation of alpha particles under the action of small-amplitude high-frequency thermal waves generated at the cavitation of a water jet on TiD targets remote from the cavitator [22, 23].

Another mechanism of reaction (1) is due to the alternative method of formation of correlated coherent states with allowance for the interaction of moving ions with atoms of the lattice. It is possible because many fast ions in the expanded laser plasma in experiments [1, 2] will move into the undestroyed crystal lattice of LiH in the channeling mode. It was shown in [16, 17] that a similar motion of comparatively slow protons in the periodic field of the lithium crystal lattice is accompanied by the very rapid formation (in the interval of three or four lattice periods) of a similar correlated coherent state of a moving particle with the correlation coefficient $1 - |r| \leq 10^{-8}$, which corresponds to the coefficient of correlation efficiency $G \geq 10^4$ and an increase in the amplitude of energy fluctuations in the transverse (with respect to the longitudinal motion) direction to the value

$$\delta E \approx \frac{(\delta p)^2}{2M} \geq \frac{G^2 \hbar^2}{8M(\delta x)^2} \approx \frac{G^2 \hbar^2}{2Ma_x^2} \geq 40 \text{ keV}, \quad (8)$$

which is many orders of magnitude higher than the energy of the longitudinal translational motion (Fig. 1). Here, M is the proton mass and $a_x \approx 2\delta x \approx 2 \text{ \AA}$ is the interplanar distance in the lattice.

This mechanism of the self-similar formation of the correlated coherent state will occur for the ions moving in the periodic field of the lattice at velocities

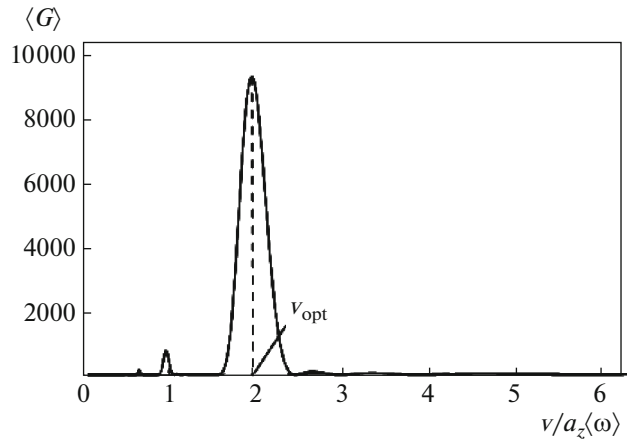


Fig. 2. Averaged coefficient of correlation efficiency versus the proton velocity at the end of the third period of the lithium lattice [16].

close to $v_{\text{opt}} \approx 2a_z\langle\omega\rangle$, which ensures the phase matching of eigenstates of the transverse quantum motion of a particle in the channel [16]. Here, $\langle\omega\rangle$ is the average frequency of oscillations of the ion between planes at channeling in the averaged potential of the walls of the channel.

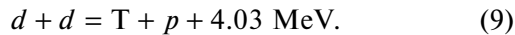
The dependence of the time-averaged quantity $\langle G \rangle$ on the velocity of protons is shown in Fig. 2. It is seen that this quantity is very large in the velocity interval approximately equal to 10% of the optimal velocity for a given crystallographic direction. The number of such particles with energies of several hundreds of electronvolts is sufficiently large in the tail of the Maxwellian distribution of ions of the laser plasma in experiments described in [1, 2].

The same mechanism (formation of the correlated coherent state at the motion of the ion in the periodic field of the lattice or in the field of a cluster of several atoms) very well describes the results of numerous experiments performed in several laboratories in the United States (Louisiana Accelerator Center in Lafayette, Physical Department of North Texas University in Deaton, and NASA MFES Center in Huntsville) with accelerated proton beams with variable energies $E \leq 500 \text{ eV}$ and two types of targets: a solid target in the form of a thin lithium foil (thickness about 1 mm) and a target in the form of saturated lithium vapor, which ensure the efficient nuclear fusion (details see in [16]).

Both above mechanisms correspond to low-energy nuclear reactions because they do not require heating or real (not virtual caused by fluctuations) acceleration of particles. They also reliably justify the complete forbiddenness [15, 17] of the channels of nuclear reactions with the fusion of initial particles and formation of radioactive compound nuclei. This forbiddenness is observed in all successful low-energy experiments and it cannot be justified by the standard methods of optimization of low-energy reactions (e.g., by means of

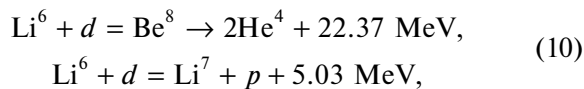
the anomalous screening of the field of the nucleus or picnonuclear effects at very strong compression of the target).

Furthermore, the analysis of the experiments reported in [1, 2] also explains a comparatively low efficiency of neutron generation ($N_{\text{neutron}}^0 \approx 10$ neutron/pulse) that was observed in these experiments. This occurs because the neutron channel $d + d = \text{He}^3 + n$ of the dd reaction, where such correlated coherent states are formed, is many orders of magnitude less probable [11, 13] than the alternative faster “proton” channel



This is due both to the specificity (duration) of reactions stimulated by virtual fluctuations of the energy and to the possible manifestation of the Oppenheimer–Phillips effect [24] associated with the mutual spatial reorientation of deuterons before their interaction leading to the capture reaction (9) without the formation of the He^4 compound nucleus.

An additional feature of the laser experiments performed in the late 1960s is that the following alternative reactions involving lithium isotopes have large probabilities in the case of the LiD target:



where products are alpha particles and protons, which should also be detected in large amount in these laser experiments. Some of the successful and efficient experiments where such measurements were performed for similar reactions with lithium and protons were considered in [16]. The implementation of reactions (10) and the detection of their products can be performed by the scheme considered in this work.

Unfortunately, the authors of the laser experiments in [1, 2] did not perform control measurements of other potentially possible products of these reactions (protons and alpha particles) with, e.g., track detectors, and these features remain unstudied and unnoticed.

4. CONCLUSIONS

The analysis of the first successful experiments on the production and study of the nuclear fusion plasma when the LiD target is irradiated by laser pulses has shown that the most probable mechanism of neutron generation is due not to the direct nuclear fusion but to the formation of correlated coherent states in the target owing to the action of the shock wave or at the motion of formed ions in the undestroyed part of the lattice of the target.

The results obtained in this work indicate the possibility of alternative reactions at the laser simulation of nuclear fusion and show that it is reasonable to more comprehensively study and to repeat this and

similar experiments in order to seek other possible products of nuclear fusion by the same method [1, 2] by means of the action of unidirectional single or repeated laser pulses. It is very important that such studies can be performed at small laboratories and do not require very comprehensive, unique, and expensive equipment, which currently exists only in a few world centers, where global problems of inertial confinement fusion are solved with the obligatory uniform compression of the target by means of time-synchronized action of laser pulses generated by many tens of ultrahigh-power lasers. Successful nuclear fusion experiments [22, 23] performed with thermal waves formed in a simple cavitation facility based on the water jet confirm the efficiency of such studies.

The above analysis also shows the necessity of certain revision of the role and efficiency of low-energy nuclear reactions for the solution of modern problems of nuclear technology. To successfully solve such problems, it is also obviously necessary not only to take into account the particular interaction between a pair of considered particles, as in high-energy nuclear physics, but also to completely analyze the effect of the environment on the efficiency of these processes. In a certain extent, this situation is similar to the well-known Mössbauer effect, where the generation of resonance gamma lines with record parameters is due both to intranuclear processes and to the properties of the environment.

REFERENCES

1. N. G. Basov, S. D. Zakharov, P. G. Kryukov, Yu. V. Senatskii, and S. V. Chekalin, PhIAS Preprint No. 63 (Lebedev Phys. Inst. Acad. Sci., Moscow, 1968).
2. N. G. Basov, S. D. Zakharov, P. G. Kryukov, Yu. V. Senatskii, and S. V. Chekalin, JETP Lett. **8**, 14 (1968).
3. N. G. Basov, S. D. Zakharov, O. N. Krokhin, P. G. Kryukov, Yu. V. Senatskii, E. L. Tyurin, A. I. Fedosimov, S. V. Chekalin, and M. Ya. Shchelev, Sov. J. Quantum Electron. **1**, 2 (1971).
4. M. M. Basko, *Physical Principles of Inertial Thermonuclear Fusion* (ITEF, Moscow, 2008) [in Russian].
5. N. Burdonskii, A. Yu. Gol'tsov, A. G. Leonov, K. N. Markarov, I. S. Timofeev, and V. N. Yufa, Vopr. At. Nauki Tekh., Ser.: Termoyad. Sintez **36** (2), 8 (2013).
6. S. I. Anisimov, A. M. Prokhorov, and V. E. Fortov, Sov. Phys. Usp. **27**, 181 (1984).
7. V. E. Fortov, *High Energy Density Physics* (Fizmatlit, Moscow, 2013; Springer, Switzerland, 2016), Par. 4.3.
8. R. Mulser and D. Bauer, *High Power Laser-Matter Interaction* (Springer, Berlin, 2010).
9. P. Mora, Phys. Fluids **25**, 1051 (1982).
10. V. I. Vysotskii and S. V. Adamenko, Tech. Phys. **55**, 613 (2010).
11. V. I. Vysotskii and M. V. Vysotskyy, Eur. Phys. J. A **49**, 99 (2013).
12. V. I. Vysotskii, S. V. Adamenko, and M. V. Vysotskyy, Ann. Nucl. Energy **62**, 618 (2013).

13. V. I. Vysotskii and M. V. Vysotskiy, *Curr. Sci.* **108**, 524 (2015).
14. V. I. Vysotskii and M. V. Vysotskiy, *J. Exp. Theor. Phys.* **125**, 195 (2017).
15. V. I. Vysotskii and M. V. Vysotskiy, *RENSIT* **9**, 21 (2017).
16. V. I. Vysotskii, M. V. Vysotskiy, and S. Bartalucci, *J. Exp. Theor. Phys.* **127**, 479 (2017).
17. S. Bartalucci, V. I. Vysotskii, and M. V. Vysotskiy, *Phys. Rev. Accel. Beams* **22**, 054503 (2019).
18. E. Schrödinger, *Ber. Kgl. Akad. Wiss.* **24**, 296 (1930).
19. H. P. Robertson, *Phys. Rev. A* **35**, 667 (1930).
20. V. V. Dodonov and V. I. Man'ko, *Tr. FIAN* **183**, 71 (1987).
21. V. V. Dodonov, A. V. Klimov, and V. I. Man'ko, *Tr. FIAN* **200**, 56 (1991).
22. A. A. Kornilova, V. I. Vysotskii, Yu. A. Sapozhnikov, I. E. Vlasova, S. N. Gaidamaka, et al., *Inzhen. Fiz.*, No. 5, 13 (2018).
23. A. A. Kornilova, V. I. Vysotskii, T. Krit, M. V. Vysotskiy, and S. N. Gaydamaka, *J. Surf. Invest.: X-ray, Synchrotr. Neutron Tech.* **14**, 117 (2020).
24. V. I. Vysotskii, *Infinite Energy* **18** (108), 30 (2013).

Translated by R. Tyapaev